Electrochemical Proton Intercalation in Vanadium Pentoxide Thin Films and its Electrochromic Behavior in the near-IR Region

Annika Buchheit,*[a] Britta Teßmer,[b] Marina Muñoz-Castro,[c] Hartmut Bracht,[c] and Hans-Dieter Wiemhöfer*[a, d]

This work examines the proton intercalation in vanadium pentoxide (V_2O_5) thin films and its optical properties in the near-infrared (near-IR) region. Samples were prepared via direct current magnetron sputter deposition and cyclic voltammetry was used to characterize the insertion and extraction behavior of protons in V_2O_5 in a trifluoroacetic acid containing electrolyte. With the same setup chronopotentiometry was done to intercalate a well-defined number of protons in the $H_xV_2O_5$ system in the range of $x=0$ and $x=1$. These films were characterized with optical reflectometry in the near-IR region (between 700 and 1700 nm wavelength) and the refractive index n and extinction coefficient k were determined using CAUCHY's dispersion model. The results show a clear correlation between proton concentration and n and k.

1. Introduction

Nowadays there is a high demand for materials with well-defined, tunable optical properties to realize new optical modulation devices, e.g. optoelectronic switches and phase or intensity modulators[1,2] as optical data processing is getting more and more important for communication and information technologies. Silicon photonic integrated circuits (PICs) are getting more and more important in this field in which the near-IR region is of great interest.[3] Recently, self-holding optical actuators for silicon photonic waveguides have been proposed, these activators can maintain the switching state without a constant supply of energy. Different types of materials have been exploited which comprise phase change,[1] insulator-metal phase transition,[4] memristor-like plasmonic structure[5] and electrochromic materials.[6]

Electrochromic materials are able to reversibly change their optical properties, i.e. refractive index and absorption coefficient by inserting charge which causes redox reactions in the material.[7] Intercalation is commonly done using lithium cations or protons since excellent reversible coloration of the materials in the visible range can be effected with these ions. Some well-known electrochromic oxides for the visible range are tungsten trioxide (WO_3),[8,9] niobium pentoxide (Nb_2O_5),[10] molybdenum trioxide (MoO_3)[11] and vanadium pentoxide (V_2O_5).[12,13,14]

V_2O_5 has been used in a broad field of different applications, for example as catalysts in oxidation reactions,[15] in sensors as gas sensing material,[16] as insertion electrodes for lithium ion batteries[17] and as already mentioned above for smart window applications as electrochromic material. There, the electrochromic effect has only been studied with lithium intercalation and in the visible range of the electromagnetic spectrum. In previous works we examined the electrochromic properties of lithiated V_2O_5 in the near-infrared (near-IR) region.[18] Nevertheless, there is only few information available regarding insertion of protons. WRUCK et al.[14] and OTTAVIANO et al.[13] describe that the insertion of a proton is possible in V_2O_5 and that it is similar to Li^+-intercalation but they only give details about the lithiation.

In 1998, a solid-state proton battery was introduced by PANDEY et al.[19] where vanadium pentoxide was used as cathode material within a mixture of carbon and lead dioxide. Therefore, it is already known that V_2O_5 may serve as a reversible proton intercalating material.

LIU et al. presented insertion of hydrogen in the form of intercalated protons accompanied by excess electrons in the conduction band of vanadium pentoxide by treating it in a hydrogen containing atmosphere.[20] In their work, they investigated the optical properties of V_2O_5 in the visible range in

[a] Dr. A. Buchheit, Prof. H.-D. Wiemhöfer
Forschungszentrum Jülich GmbH
Helmholtz Institute Münster, IEK 12
Corrensstr. 46
48149 Münster (Germany)
E-mail: a.buchheit@fz-juelich.de
h.wiemhoefer@fz-juelich.de
[b] B. Teßmer
University of Münster
MEET Battery Research Centre
Corrensstr. 46
48149 Münster (Germany)
[c] Dr. M. Muñoz-Castro, Prof. H. Bracht
Institute of Materials Physics
Wilhelm-Klemm-Str. 10
48149 Münster (Germany)
[d] Prof. H.-D. Wiemhöfer
University of Münster
Institute of Inorganic and Analytical Chemistry
Corrensstr. 28/30
48149 Münster (Germany)

ChemistryOpen

Full Papers
doi.org/10.1002/open.202000267

Chemistry Europe
European Chemical
Societies Publishing

dependence of the hydrogen content in the gas mixture in a Pd/V_2O_5 device. Thus, they showed that vanadium pentoxide irreversibly changes in a first formation cycle of insertion and extraction of hydrogen but then remains optically passive for the subsequent cycles. By electrochemical insertion of protons, V_2O_5 has never been tested before as an optically active and tunable material.

In 2013, MALINI et al. presented electrochromism of thin films of $CeVO_4$, a mixed oxide sythesized from cerium dioxide and vanadium pentoxide.[21] They inserted and extracted protons electrochemically via hydrochloric acid containing electrolyte and measured the transmittance in the ultraviolet and visible range *in-situ*. They showed that there is a decrease of the transmittance with rising H^+ content, giving a clear hint that V_2O_5 can act as an electrochromic active material.

To conclude, previous research has been focused on characterizing the electrochromism of vanadium pentoxide mainly in relation to lithiation, there is still a lack of information about the electrochromic properties of pure vanadium oxide with electrochemical proton intercalation especially in the near-IR region. Accordingly, it is of interest to investigate the electrochromic behavior as a function of concentration of intercalated protons.

Therefore, we prepared vanadium pentoxide thin films via direct current magnetron sputter deposition and investigated in detail their electrochemical and electrochromic properties in the near-IR region in terms of proton insertion and extraction.

2. Results and Discussion

The sputtered and annealed V_2O_5 films all exhibit an ortho-rhombic structure well matching literature data.[22] An x-ray diffraction (XRD) spectrum of an as prepared V_2O_5 film (600 nm thickness) on bare silicon is presented in Figure 1. No representative reflex of vanadium dioxide (VO_2)[23] can be found so we conclude that all produced thin films consist of pure crystalline V_2O_5.
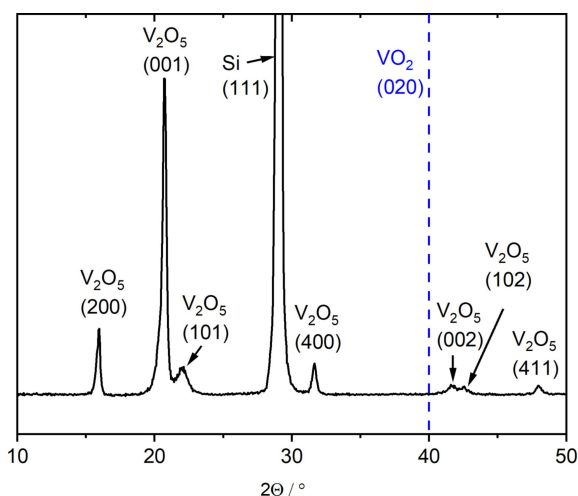
In a next step we investigated the electrochemical performance in a proton containing electrolyte. Therefore, we have chosen trifluoroacetic acid in a solution of tetrabutylammonium perchlorate in propylene carbonate for the following reasons: In contrast to many other acid solutions, this composition does not dissolve the V_2O_5 thin film. Nevertheless, trifluoroacetic acid is a strong acid with a pK_a-value of 0.23,[24] its solubility in various organic solvents is excellent and in our case it is serving as proton source. Tetrabutylammonium perchlorate is needed as conducting salt to guarantee good conductivity of our electrolyte system, whereupon especially the cation is too big to be intercalated in the structure of V_2O_5. As solvent propylene carbonate was chosen, because it is a well-known solvent for electrolytes in lithium-ion batteries,[25] exhibiting good electrochemical stability.

According to OTTAVIANO et al.[13] and TONG et al.,[26] in an electrochemical experiment the intercalation and deintercalation mechanism of protons in V_2O_5 can be described as

$$V_2O_5 + xH^+ + xe^- \rightleftharpoons H_xV_2O_5.$$
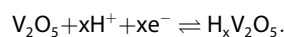
While intercalating a proton, V^{5+} is reduced to V^{4+} and the proton should coordinate with the oxygen atom to form a hydroxyl species.

Figure 2 shows a cyclic voltammetry (CV) measurement of a V_2O_5 thin film (1.2 μm thickness) in the voltage range between 0.1 and 1.3 V versus silver chloride electrode (Ag|AgCl) and a scan rate of 1 mV·s^{-1}. A well-defined reduction peak and two oxidation peaks are observable, which indicate that at least the deintercalation of protons is taking place in a two-step mechanism, whereas a second peak in the reduction area could not be observed.

The overall coulombic efficiency of the system is 89%, indicating that the intercalation and deintercalation process is not fully reversible. This assumption is supported by the fact that the peak current densities are decreasing with repeated cycling. Regarding the relatively high number of protons
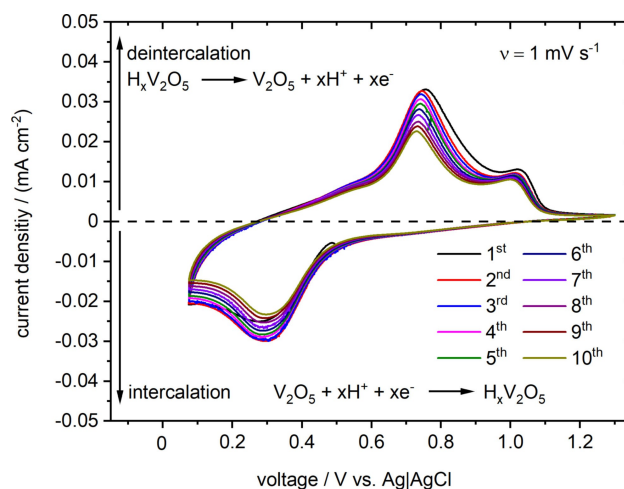

Figure 1. XRD spectrum of a V_2O_5 thin film on a bare silicon wafer.

Figure 2. CV of a V_2O_5 thin film (1.2 μm) with 0.1 molal trifluoroacetic acid and 0.4 molal tetrabutylammonium perchlorate in propylene carbonate as electrolyte, Pt as counter electrode and Ag|AgCl as reference for 10 cycles.

ChemistryOpen

Full Papers
doi.org/10.1002/open.202000267

Chemistry Europe
European Chemical
Societies Publishing

intercalated ($x = 0.5$ according to calculated flowed charge) in one cycle of the CV, reversible intercalation and deintercalation of protons could still be possible by focusing on smaller values of x.

For this purpose, a 300 nm thin film of V_2O_5 was investigated with chronopotentiometry. The film was reversibly loaded with ± 0.5 µA to a state corresponding to $H_{0.05}V_2O_5$ and back to $H_0V_2O_5$ for 40 cycles. After a total of five formation cycles the complete system reacts reversible by constantly ranging between 1.15 V (deintercalated, $x = 0$) and 0.55 V (intercalated, $x = 0.05$) vs. Ag|AgCl, as shown in Figure 3. By this means, repeated cycling of vanadium oxide films in proton conducting electrolyte has proven to be fully reversible in a well-defined range of x at least to $x = 0.05$. Comparable results can also be obtained for higher constant currents up to 50 µA, which enables faster switching between different values of x (in the case of a 300 nm thick 1×1 cm film less than one minute), making $H_xV_2O_5$ a promising system for switches or tuning devices. Graphs of chronopotentiometry measurements done with higher currents than 0.5 µA (5 µA and 50 µA) can be found in the supplementary data.

After proving the electrochemical functionality of the $H_xV_2O_5$ system, the optical behavior of the thin films was investigated as a function of the proton content. Therefore, chronopotentiometry was used with a constant current of ± 0.5 µA for a well-defined period of time to set an accurate value of x, before and after each experiment the cell voltage was measured until open circuit potential (OCP) was reached (OCP values see Table 1). Between every intercalation and
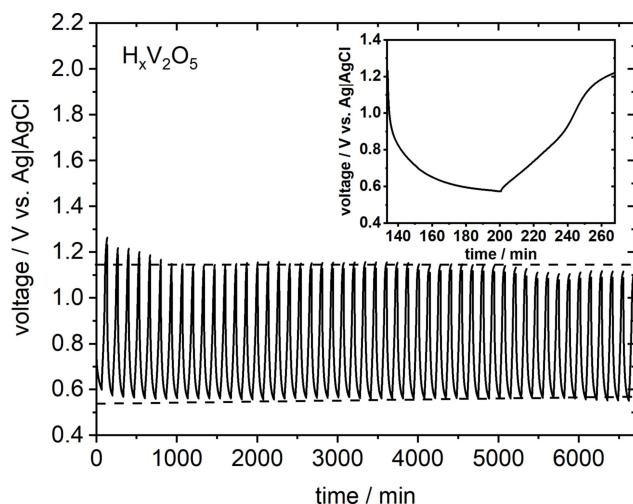
deintercalation the cell was dismounted and the thin film was cleaned with ethanol. The sample was investigated with reflectance spectroscopy before and after the intercalation and additionally after the deintercalation.

Figure 4 shows two chronopotentiometry graphs, one for the intercalation and one for deintercalation. The belonging reflectance graphs of the same sample with $x = 0$, $x = 0.1$ and deintercalated back to $x = 0$ are also shown in the same figure. It is visible that there is a definite deviation between intercalated and the deintercalated state. Furthermore, a very good reversibility of the intercalation and deintercalation process is evident since the reflectance spectrum after the deintercalation step matches very well to the spectrum measured before intercalation. This also proves the reversibility of the electrochemical process up to $x = 0.1$.

Not only the reversibility, but also the stability or the maintaining of the optical properties of the intercalated state is of great importance for use as an optical switch. Therefore, a sample of $H_0V_2O_5$ was intercalated to $H_{0.1}V_2O_5$, the sample was cleaned and the reflectance was measured directly afterwards. Then, the sample was allowed to rest in ambient conditions, whereas the reflectance was measured after six, nine and twenty days. In Figure 5 the reflectance curves are shown and it is observable that the reflectance changed a little bit between the freshly intercalated sample and the curve measured after six days. One reason for this could be the non-ideal cell-setup, as it was not possible to contact the whole area of the V_2O_5 thin film with liquid electrolyte without directly contacting the current collector (see also in Figure 7). It is assumed that shortly after intercalation the layer is not yet in total equilibrium. This is also the reason why we decided not to examine the time response of the thin films with additional chronoamperometric measurements. Nevertheless, the reflectance curves after six, nine and twenty days are in good accordance to each other, no change in the reflectivity can be seen on further storage. Thus, the intercalated films are stable for the whole period of 20 days and
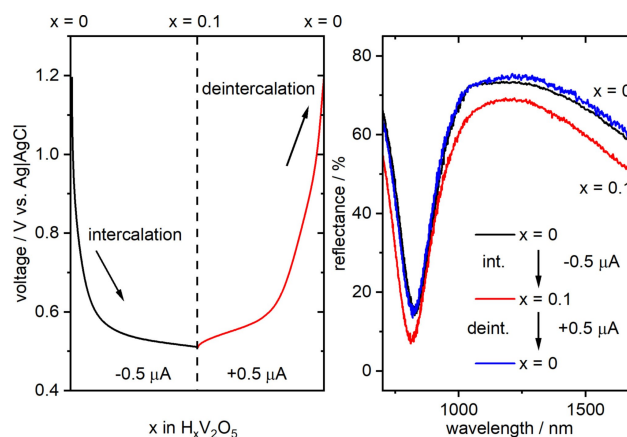
Figure 3. Chronopotentiometric cycling of a V_2O_5 thin film (300 nm) for 40 cycles; applied current ± 0.5 µA; load capacity of H^+ $x = 0.05$.

Table 1. OCP values of the cell with V_2O_5 thin film as working electrode, Pt as counter electrode and Ag|AgCl as reference.

x in $H_xV_2O_5$	OCP vs. Ag|AgCl
0	1.20 ± 0.12 V
0.05	0.54 ± 0.04 V
0.1	0.48 ± 0.02 V

Figure 4. Left: Chronopotentiometry of a $H_xV_2O_5$ thin film from $x = 0$ to $x = 0.1$ and back to $x = 0$. Right: Reflectance measurement of the intercalated and deintercalated sample. Proton insertion shows a significant effect on the optical properties, while proton extraction allows returning to the state of $x = 0$.
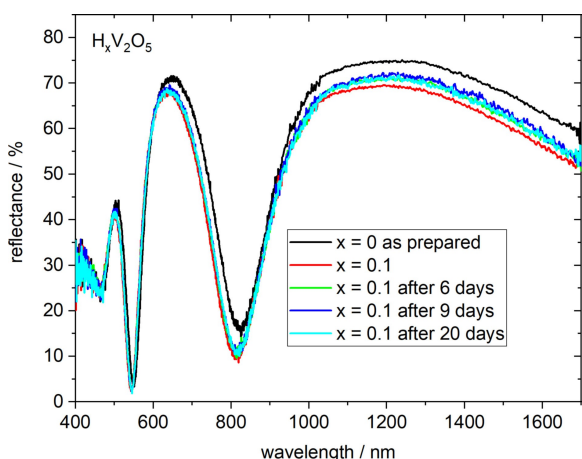
ChemistryOpen

Full Papers
doi.org/10.1002/open.202000267

Chemistry Europe
European Chemical
Societies Publishing

Figure 5. Reflectivity spectra of a $H_xV_2O_5$ thin film which was intercalated to $x = 0.1$. The sample was then stored at ambient conditions for several days.

are able to maintain their optical properties in the intercalated phase.

In a next step we investigated if a systematic trend in the change of the optical properties can be seen by varying the concentration of protons. For this reason, the sample was intercalated to a certain amount of x in several steps from $x = 0$ to $x = 1$. Between the intercalations the sample was always taken out of the electrochemical cell and the reflectance was measured. We discovered that there is a clear correlation between the number of protons intercalated in the V_2O_5 thin film and the optical properties which can be seen in Figure 6 (for small proton concentrations, $x = 0.02$ to $x = 0.08$ see the supporting information).

Overall, the reflectance decreases with increasing proton concentration. In addition, the maxima and minima of the reflectance curves are shifted to lower wavelengths on the x-axis indicating a change in the refractive index n value with proton intercalation. The intercalation and deintercalation
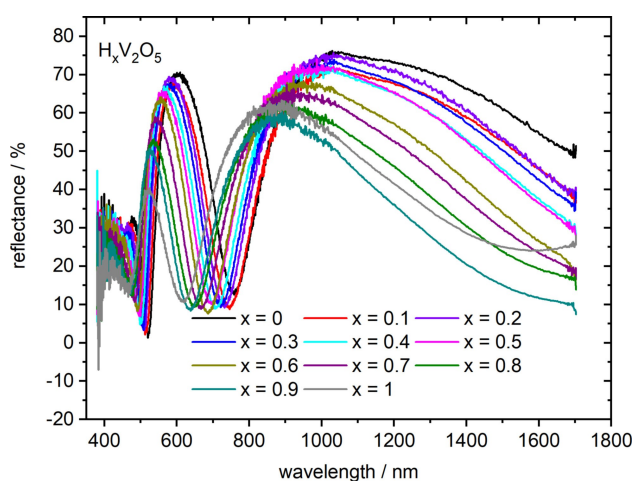
process is reversible up to a proton concentration of $0.1 < x < 0.2$. With higher amounts, the reflectance graph of the proton free state ($x = 0$) cannot be obtained anymore and is shifted to lower reflectance values (reflectance graphs are shown in the supporting information). Figure 7 gives an impression of the irreversible change of the optical properties in the visible range of the spectrum, showing photographs of a $H_xV_2O_5$ thin film sample without protons and with a proton concentration of $x = 0.2$ and $x = 0.6$. There is a clear color change observable in the whole area where the sample was in direct contact with the electrolyte. It was impossible to reach the initial state again. In the following the focus is concentrated on lower amounts of x, namely in the range between $x = 0$ and $x = 0.2$ to stay in the reversible range of intercalation, which is especially interesting for optical devices.

To determine the refractive index n and the absorption coefficient k of the measured samples, CAUCHY's dispersion model was used according to equations (3) and (4). Figure 8 shows the CAUCHY fit for a reflectance measurement done on a V_2O_5 thin film with a proton concentration of $x = 0.1$. As can be seen the fit accuracy is excellent and reaches a goodness of fit value higher than 99%. The received graphs for the n and k values dependent on the wavelength are presented in the inset. It is observable that the values for the refractive index n are
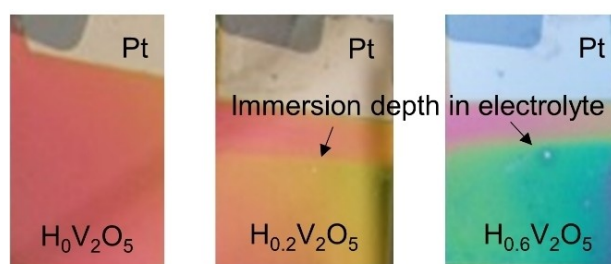

Figure 7. $H_xV_2O_5$ thin films (300 nm) with different amounts of protons inserted (from left to right: $x = 0$, $x = 0.2$ and $x = 0.6$). The area of sputtered V_2O_5 is approximately 1×1 cm.

Figure 6. Reflectance measurement of a $H_xV_2O_5$ thin film (300 nm) with different amounts of protons inserted. Small values of x ($x = 0.02-0.08$) are not shown due to clarity.
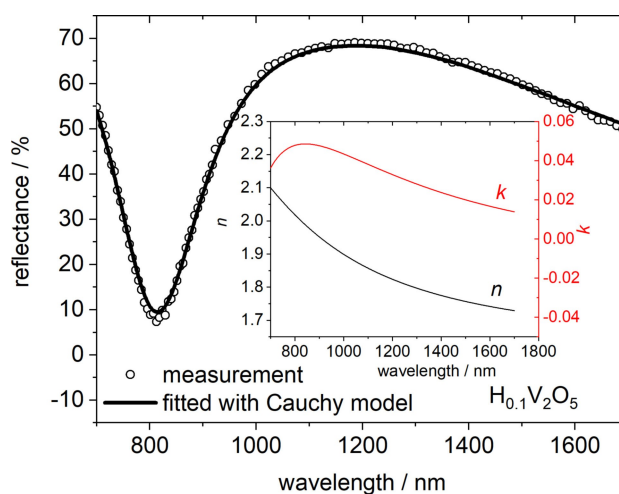

Figure 8. Reflectance data of $H_{0.1}V_2O_5$ fitted with CAUCHY model resulting in a goodness of fit higher than 99%; the inlet shows the resulting n and k graphs.
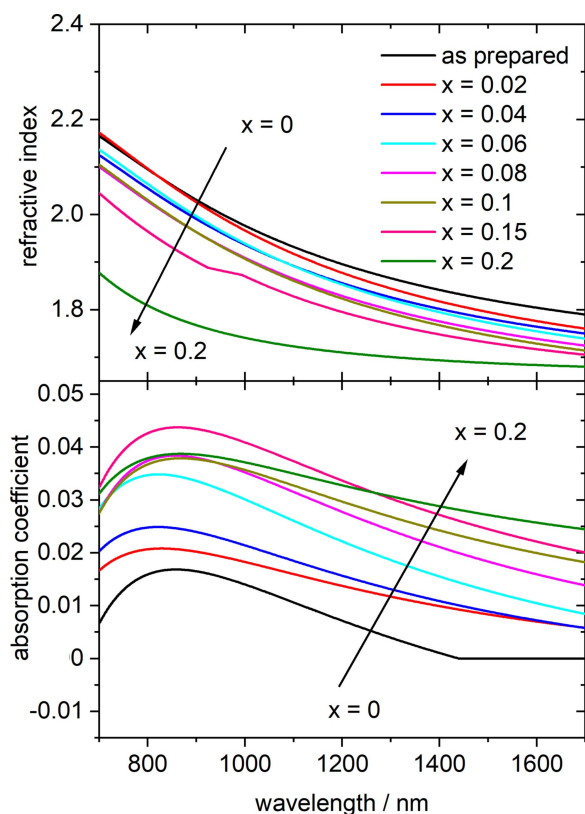
ChemistryOpen

Full Papers
doi.org/10.1002/open.202000267

Chemistry Europe
European Chemical
Societies Publishing

Figure 9. n and k values of $H_xV_2O_5$ films in the range of $x=0$ and $x=0.2$ fitted with Cauchy model.
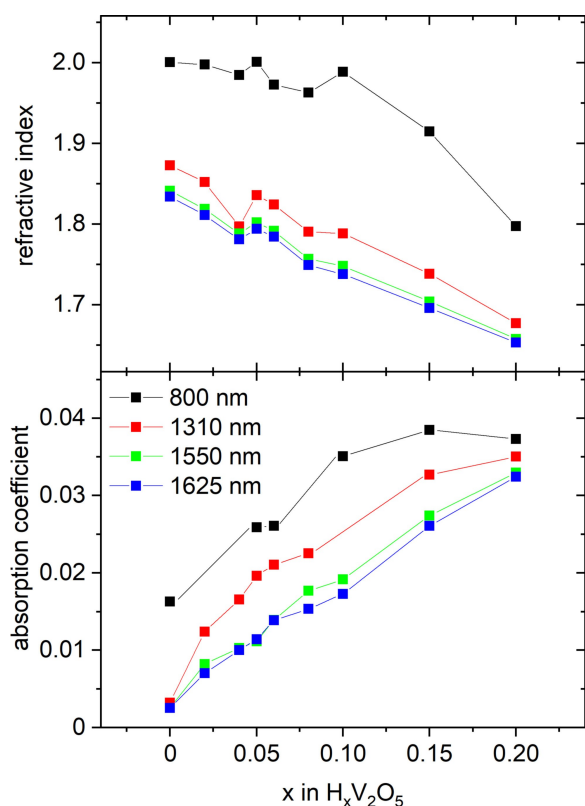

Figure 10. n and k values in dependence of proton concentration in $H_xV_2O_5$ for different wavelengths relevant for telecommunication purposes.

constantly decreasing in a wavelength range between 700 and 1700 nm while the graph of the absorption coefficient k exhibits a maximum at 850 nm. At higher wavelengths, the values are also decreasing. According to this example of fitting all other measured reflectance graphs were evaluated.

The obtained graphs for n and k are summarized in Figure 9, where it can be seen that there are just results for samples with a number of intercalated protons between $x=0$ and $x=0.2$. Beyond that no additional values for n and k could be obtained. It is noticeable that the limit of reversibility was determined between $0.1 < x < 0.2$ and the reflectance curves can only be fitted up to $x=0.2$, whereas the goodness of fit is dramatically decreased for $x=0.2$. The shape of the obtained curves of n and k in dependence of the wavelength is comparable for all values of x and a clear trend can be observed. The n curves are decreasing with increasing wavelengths. A maximum for k is observable before the values are also decreasing with increasing wavelength for all obtained data curves of different intercalated amounts of x. In general, the refractive index n is decreasing with higher amounts of x incorporated in the structure of V_2O_5 and the absorption coefficient k is increased.

This trend can be seen more clearly by plotting the n and k values against the x values of $H_xV_2O_5$ for different wavelengths (cf. Figure 10). There, a nearly linear behavior of both n and k is clearly visible. For comparison with literature values of e.g. lithiated V_2O_5, it is helpful to determine $\triangle n/\triangle x$ and $\triangle k/\triangle x$ at a distinguished wavelength. According to[18] $\triangle n/\triangle x$ is -1 and $\triangle k/\triangle x$ is 1.43 for $Li_xV_2O_5$ at a wavelength of 1550 nm. For our investigated system $H_xV_2O_5$ $\triangle n/\triangle x$ is round about -0.93 and $\triangle k/\triangle x$ round about 0.15 at the same wavelength. Comparing both systems, the change in n is a little bit lower for $H_xV_2O_5$, but in the same order of magnitude, whereas the change in k is smaller for $H_xV_2O_5$.

3. Conclusions

V_2O_5 thin films were successfully prepared with dc magnetron sputter deposition and following annealing. It has been proven that V_2O_5 is an excellent material for electrochemical proton intercalation and that the system $H_xV_2O_5$ can be used as an electrochromic cathodic material in the near-IR region. The reflectivity and therefore the n and k values of the material can be influenced systematically with proton insertion. The behavior of $H_xV_2O_5$ is comparable with $Li_xV_2O_5$[18] although the absolute change of the optical constants, especially the absorption coefficient k, is smaller with proton intercalation than with lithiation. However, one advantage over $Li_xV_2O_5$ is that it is easier to handle in non-inert environments, as there is no need for moisture-sensitive materials like metallic lithium. To conclude, $H_xV_2O_5$ is a material which is excellent for use in future optical devices.

ChemistryOpen

Full Papers
doi.org/10.1002/open.202000267

Chemistry Europe
European Chemical
Societies Publishing

Experimental Section

Thin Film Preparation

V_2O_5 thin films were prepared by dc magnetron sputter deposition. A two-inch vanadium metal target (HMW Hauner, 99.95% purity) was used with additional oxygen as the reactive gas component. Polished silicon (111) wafers with a 100 nm sputtered platinum layer were used as substrates. Before the deposition of V_2O_5, the sputter chamber (Bestec) was evacuated to a base pressure of 10^{-8} mbar and the vanadium metal target was pre-sputtered in argon for 60 s to get rid of possible impurities on the target surface. Afterwards the Ar/O_2 ratio was fixed to 40% oxygen content and the total working pressure was set to $5 \cdot 10^{-3}$ mbar. For the deposition of V_2O_5, a dc sputtering power of 2.4 W·cm^{-2} was used. These parameters resulted in a sputter rate of 1.5 nm·min^{-1} of V_2O_5. After sputtering, the obtained V_2O_5 thin films were annealed at 250 °C for 24 h to ensure crystalline structure. Verifying structure and stoichiometry, XRD measurements were done using a D5000 X-ray diffractometer (Siemens) in $\theta/2\theta$ configuration with Cu K$_\alpha$ radiation and an angular resolution of 0.05°·s^{-1}. To determine the thickness of the samples, a Dektak XT stylus profilometer (Bruker) was used.

Electrochemical Measurements

Cyclic voltammetry (CV) and chronopotentiometry measurements were performed to investigate the electrochemical behavior of the V_2O_5 thin films and the insertion/extraction properties of H$^+$ in V_2O_5 layers in a proton containing electrolyte. Therefore, a standard three-electrode-setup was used consisting of the V_2O_5 sample as working electrode (the Pt layer underneath served as current collector) and a Pt foil (chempur, 99.9% purity) as counter electrode. As reference an Ag│AgCl reference electrode (EDAQ ET072) was used. Thus, all potentials in this paper are given versus Ag│AgCl. A solution of 0.1 mol·kg^{-1} trifluoroacetic acid (Acros Organics, 99.0% purity) and 0.4 mol·kg^{-1} tetrabutylammonium perchlorate (Sigma Aldrich, 98.0% purity) in propylene carbonate (Merck SelectiLyte®, 99.9% purity) served as electrolyte, slightly modified after Dini et al.[8] All electrochemical experiments were carried out with an Autolab PGSTAT302 N (Metrohm) potentiostat at room temperature. For the chronopotentiometric measurements, a constant electric current of ±0.5 µA was applied to the samples to be examined, whereupon the amount of intercalated protons x is correlated with the inserted charge Q according to $x = \frac{Q \cdot M}{e \cdot \rho \cdot A \cdot d \cdot N_A}$ (1), being M the molar mass, e the elementary charge, ρ the density of V_2O_5, d the thickness and A the area of the film and N_A the Avogadro constant.

Optical Characterization

Optical properties of the protonated and deprotonated V_2O_5 thin films were determined using a F40-EXR reflectance spectrometer (Filmetrics) within a wavelength range between 400 and 1700 nm. A tungsten halogen lamp served as light source, whereby a beam of the light was focused on the sample surface with a spot size of 289 µm^2. For determination of the complex refractive index $n'(\lambda) = n(\lambda) + i \bullet k(\lambda)$ (2), Cauchy's dispersion model was used according to $n(\lambda) = A_n + \frac{B_n}{\lambda^2} + \frac{C_n}{\lambda^4}$ (3) and $k(\lambda) = A_k + \frac{B_k}{\lambda^2} + \frac{C_k}{\lambda^4}$ (4) whereas n is the real part (refractive index), k is the imaginary part (absorption coefficient) of the complex refractive index. A, B, and C are the Cauchy parameters and λ the wavelength.

Conflict of Interest

The authors declare no conflict of interest.

[1] D. Tanaka, Y. Ikuma, Y. Shoji, M. Kuwahara, X. Wang, K. Kintaka, H. Kawashima, T. Toyosaki, H. Tsuda, *Electron. Lett.* **2011**, *47*, 268.

[2] Y. Zhang, X. Zhang, Y. Huang, C. Huang, F. Niu, C. Meng, X. Tan, *Solid State Commun.* **2014**, *180*, 24.

[3] a) M. Asghari, A. V. Krishnamoorthy, *Nat. Photonics* **2011**, *5*, 268; b) J. Leuthold, C. Koos, W. Freude, *Nat. Photonics* **2010**, *4*, 535; c) M. Heck Jr, H.-W. Chen, A. W. Fang, B. R. Koch, D. Liang, H. Park, M. N. Sysak, J. E. Bowers, *IEEE J. Sel. Top. Quantum Electron.* **2010**, *17*, 333; d) M. Lipson, *J. Lightwave Technol.* **2005**, *23*, 4222.

[4] L. D. S. Diana, F. C. Juan, A. R. Escutia, P. S. Kilders, *J. Opt.* **2017**, *19*, 35401.

[5] C. Hoessbacher, Y. Fedoryshyn, A. Emboras, A. Melikyan, M. Kohl, D. Hillerkuss, C. Hafner, J. Leuthold, *Optik* **2014**, *1*, 198.

[6] M. Muñoz-Castro, N. Walter, J. K. Prüßing, W. Pernice, H. Bracht, *ACS Photonics* **2019**, *6*, 1182.

[7] C. G. Granqvist, *Handbook of inorganic electrochromic materials*, Elsevier, **1995**.

[8] D. Dini, F. Decker, E. Masetti, *J. Appl. Electrochem.* **1996**, *26*, 647.

[9] a) A. Hjelm, C. G. Granqvist, J. M. Wills, *Phys. Rev. B* **1996**, *54*, 2436; b) C. G. Granqvist, *Appl. Phys. A* **1993**, *57*, 3; c) C.-G. Granqvist, G. A. Niklasson, A. Azens, *Appl. Phys. A* **2007**, *89*, 29; d) S. Green, J. Backholm, P. Georén, C.-G. Granqvist, G. A. Niklasson, *Sol. Energy Mater. Sol. Cells* **2009**, *93*, 2050.

[10] a) D. D. Yao, R. A. Rani, A. P. O'Mullane, K. Kalantar-zadeh, J. Z. Ou, *J. Phys. Chem. C* **2013**, *118*, 476; b) Z. -W Fu, J. -J Kong, Q. -Z Qin, *J. Electrochem. Soc.* **1999**, *146*, 3914.

[11] a) S.-H. Lee, M. J. Seong, C. E. Tracy, A. Mascarenhas, J. R. Pitts, S. K. Deb, *Solid State Ionics* **2002**, *147*, 129; b) Y. A. Yang, Y. W. Cao, B. H. Loo, J. N. Yao, *J. Phys. Chem. B* **1998**, *102*, 9392.

[12] a) M. Benmoussa, A. Outzourhit, A. Bennouna, E. L. Ameziane, *Thin Solid Films* **2002**, *405*, 11; b) A. Cremonesi, D. Bersani, P. P. Lottici, Y. Djaoued, R. Brüning, *Thin Solid Films* **2006**, *515*, 1500; c) A. Talledo, C. G. Granqvist, *J. Appl. Phys.* **1995**, *77*, 4655.

[13] L. Ottaviano, A. Pennisi, F. Simone, A. M. Salvi, *Opt. Mater.* **2004**, *27*, 307.

[14] D. Wruck, S. Ramamurthi, M. Rubin, *Thin Solid Films* **1989**, *182*, 79.

[15] R. Ramirez, B. Casal, L. Utrera, E. Ruiz-Hitzky, *J. Phys. Chem.* **1990**, *94*, 8960.

[16] a) D. Manno, A. Serra, M. Di Giulio, G. Micocci, A. Taurino, A. Tepore, D. Berti, *J. Appl. Phys.* **1997**, *81*, 2709; b) N. Izu, G. Hagen, D. Schönauer, U. Röder-Roith, R. Moos, *Sensors* **2011**, *11*, 2982.

[17] a) D. McNulty, D. N. Buckley, C. O'Dwyer, *J. Power Sources* **2014**, *267*, 831; b) A. -M Cao, J.-S. Hu, H.-P. Liang, L.-J. Wan, *Angew. Chem. Int. Ed.* **2005**, *44*, 4391; c) S. Wang, Z. Lu, D. Wang, C. Li, C. Chen, Y. Yin, *J. Mater. Chem.* **2011**, *21*, 6365; d) C. R. Sides, C. R. Martin, *Adv. Mater.* **2005**, *17*, 125.

[18] M. Muñoz-Castro, F. Berkemeier, G. Schmitz, A. Buchheit, H.-D. Wiemhöfer, *J. Appl. Phys.* **2016**, *120*, 135106.

[19] K. Pandey, N. Lakshmi, S. Chandra, *J. Power Sources* **1998**, *76*, 116.

[20] a) P. Liu, S.-H. Lee, H. M. Cheong, C. E. Tracy, J. R. Pitts, R. D. Smith, *J. Electrochem. Soc.* **2002**, *149*, H76–H80; b) P. Liu, S.-H. Lee, C. E. Tracy, J. A. Turner, J. R. Pitts, S. K. Deb, *Solid State Ionics* **2003**, *165*, 223.

[21] D. R. Malini, C. Sanjeeviraja, *Int. J. Electrochem. Sci.* **2013**, *8*, 1349.
[22] a) A. Bystrom, K. A. Wilhelmi, O. Brotzen, *Acta Chem. Scand.* **1950**, *4*, 1119; b) J. Haber, M. Witko, R. Tokarz, *Appl. Catal. A* **1997**, *157*, 3.
[23] J. F. de Natale, P. J. Hood, A. B. Harker, *J. Appl. Phys.* **1989**, *66*, 5844.
[24] C. W. Klampfl, W. Ahrer, *Electrophoresis* **2001**, *22*, 1579.
[25] a) R. Wagner, S. Brox, J. Kasnatscheew, D. R. Gallus, M. Amereller, I. Cekic-Laskovic, M. Winter, *Electrochem. Commun.* **2014**, *40*, 80; b) H. Zhao, S.-J. Park, F. Shi, Y. Fu, V. Battaglia, P. N. Ross, G. Liu, *J. Electrochem. Soc.* **2014**, *161*, A194–A200.

[26] Z. Tong, J. Hao, K. Zhang, J. Zhao, B.-L. Su, Y. Li, *J. Mater. Chem. C* **2014**, *2*, 3651.